Atomistically Modeling the Chemical Potential of Small Molecules in Dense Polymer Microstructures. 2. Water Sorption by Polyamides

Birgitta Knopp and Ulrich W. Suter*

Department of Materials, Institute of Polymers, ETH (Swiss Federal Institute of Technology), CH-8092 Zürich, Switzerland

Received March 19, 1997; Revised Manuscript Received July 10, 1997[⊗]

ABSTRACT: The solution thermodynamics of water in dense amorphous polyamide structures are assessed. Amorphous microstructures of polyamide(6) (PA-6), polyamide(12) (PA-12), and a copolyamide of hexamethylenediamine and isophthalic acid (PA-6I) are generated according to the amorphous-cell methodology on an atomistically detailed level. Applying a combination of thermodynamic integration and Widom's particle-insertion method to systems containing different numbers of water molecules yields estimates of the excess chemical potential of water dissolved in the polymer systems. The degree to which the polymers favor the absorption of water from their environment can be assessed and it is in reasonable agreement with experimental values for the equilibrium water contents.

Introduction

Understanding the equilibrium sorption of gases, vapors, and liquids in polymers is important in many areas of polymer technology such as design of barrier and separation membranes, packaging, and polymer processing. It is, therefore, desirable to be able to use molecular modeling to investigate the sorption behavior of polymer materials. Recently, many computational studies of the permeation of small gas molecules through polymer membranes have appeared that were designed to analyze, on an atomistic scale, diffusion mechanisms or to calculate the diffusion coefficient and solubility parameter.[1−18] Solubilities of small molecules in polymer materials were mainly calculated by particle-insertion techniques and, therefore, limited to small, simple gas molecules. Up to now, these calculations correctly described the ordering of solubilities among different gases.

However, except for the simplest compounds,[7] the absolute Henry constants calculated exceed the corresponding experimental values by 1−2 orders of magnitude.[3,11] This disagreement has been attributed to an error of (2−4) kT commonly found in calculations of Helmholtz energies by molecular dynamic (MD) simulations[10] or, after detailed examination of the polymer microstructures, to the fact that the main contribution to the solubility is provided by single holes in the simulated polymer structure, which might not be present in similar proportion in real amorphous polymers.[11] The strong dependence of the solubility on the detailed polymer microstructure under investigation and the fact that more sophisticated methods for the polymer structure generation (slow compression with soft-core potentials or repulsive potentials) seem to be able to improve the results obtained for the solubility of light gases in amorphous polymers support this viewpoint.[19] Nevertheless, the extension of the solubility calculations to larger molecules or small molecules exhibiting long-range interactions has not yet succeeded.

It is the aim of this study to demonstrate the applicability of the two-step method described in the preceding paper in this issue.[20] There, it was shown that calculation of the excess chemical potential of water in dense polymer microstructures is possible. Here, we chose three different polyamide systems, poly(imino-1-oxohexamethylene) (PA-6), poly(imino-1-oxododecamethylene) (PA-12), and a copolyamide of hexamethylenediamine and isophthalic acid (1:1) (PA-6I) to investigate their water sorption behavior. The systems were chosen because it is well-known that polyamides may contain considerable amounts of water, depending on the environment. Since the crystalline regions of polymers are generally assumed to be inaccessible to penetrants, we restrict our considerations to purely amorphous structures.

The sorption behavior of the polyamide/water systems can be analyzed by estimating the excess chemical potential of water dissolved in the polymer microstructure containing different numbers of water molecules. We consider the cases of polymer submerged in neat water. In equilibrium, the excess chemical potential of the water dissolved in the polymer microstructure then equals the excess chemical potential of pure water and the difference between these values,

$$\Delta\mu^{\mathrm{ex}} = \mu^{\mathrm{ex}}_{(\text{water in polymer})} - \mu^{\mathrm{ex}}_{(\text{pure water})} \qquad (1)$$

vanishes. A negative difference in the excess chemical potentials indicates that the polymer likes to absorb more water from the environment; the opposite signals the existence of a thermodynamic barrier against further water sorption. The key property, the excess chemical potential of water dissolved in the polymer matrix, is calculated here using a combination of thermodynamic integration and Widom's particle-insertion method, as described in detail in the companion paper[20] and sketched in Figure 1. We emphasize that in all calculations reported here, the internal degrees of freedom of the water molecules are fully taken into account.

Simulation Details

All calculations on various polyamide/water systems were performed either on IBM RS6000 or SGI INDIGO2 workstations using the standard steepest descent minimization algorithm and NVT and NpT molecular dynamic (MD) algorithms.[21] The MD simulations were carried out using Berendsen's thermostat[22] to control

[⊗] Abstract published in *Advance ACS Abstracts,* September 1, 1997.

S0024-9297(97)00384-7 CCC: $14.00

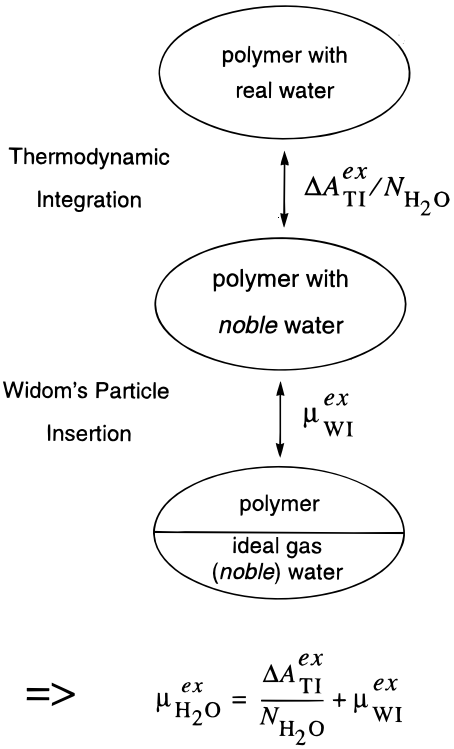

Figure 1. Schematical illustration of the system stages during the calculation.

the temperature during data sampling. The equations of motion were integrated with the Verlet leapfrog integrator[23] and a time step of 1 fs. A modified version of the *pcff* force field[20,21] was used to describe the interactions at a fully atomistic level, including internal degrees of freedom for all molecules, polymer as well as water. The nonbonded interactions, i.e., Lennard-Jones and Coulombic interactions, were truncated at 8.5 Å using a fifth-order spline from 7.5 to 8.5 Å. Preliminary studies, not described here, on PA-6 had shown this relatively small "cutoff" to be appropriate for this system, even though it is applied to the long-range Coulombic interaction. Periodic continuation conditions and the minimum-image convention applied to all simulations.

The solubility calculations were carried out on amorphous polyamide/water systems built of one polymer chain (consisting of 50, 30, and 30 monomeric units for PA-6, PA-12, and PA-6I, respectively) and a number of water molecules that were chosen according to the desired water content of the system. The polymer/water structures were generated using an RIS-based "amorphous-cell" scheme.[21,24] The initial densities were set corresponding to the densities of the dry amorphous polymer species at 300 K.[25,26] A detailed overview of all polyamide/water systems investigated is given in Table 1. For the PA-6 system containing 20 wt % water and the PA-12 system containing 2 wt % water, three independent structures each were generated to investigate the influence of the variability of the initial polymer structure.

After 1000 steps of steepest-descent minimization of the total potential energy with respect to the coordinates of all atoms in the systems, all initial polyamide/water structures were equilibrated for 50 ps with MD simulation under constant *NVT* conditions. Further equilibration and density adjustment were achieved by an additional MD run for 350 ps under constant *NpT* conditions using Berendsen's method,[22] which couples the system to a "pressure bath" maintained at a certain

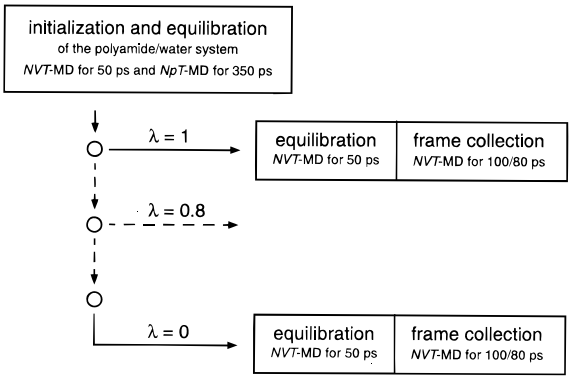

Figure 2. Overview of the simulation procedure, carried out with each polyamide/water system.

Table 1. Overview of the Initial System Parameters of the Polyamide/Water Systems Investigated

	water content (wt %)	no. of water molecules	box edge (Å)	cutoff correction pressure (bar)
PA-6, $X = 50$, $\rho^{dry}_{amorphous} = 1.09$ g/cm^3	5	17	20.87	1341
	10	35	21.24	1340
	15	55	21.64	1340
	20	79	22.10	1340
	25	105	22.57	1340
	30	135	23.10	1340
	50	314	25.83	1339
PA-12, $X = 30$, $\rho^{dry}_{amorphous} = 1.01$ g/cm^3	2	7	21.50	1211
	5	17	21.72	1210
	10	37	22.13	1206
	20	82	23.00	1200
	30	141	24.05	1193
PA-6I, $X = 30$, $\rho^{dry}_{amorphous} = 1.18$ g/cm^3	5	22	22.21	1579
	10	46	22.62	1578
	15	72	23.04	1578
	20	102	23.51	1577
	25	137	24.03	1577
	30	176	24.59	1576

target pressure. During the constant-*NpT* equilibration, a constant external pressure was applied to the system to compensate for the long-range forces neglected by the splined cutoff.

The last configuration of the equilibration of each run was used as the initial configuration for the subsequent MD runs with the different λ-dependent force fields that are necessary for the thermodynamic integration. These structures were again equilibrated over 50 ps *NVT*-MD in order to adapt to force field changes; then 100 configurations (in the case of PA-6 and PA-6I) and 80 configurations (in case of PA-12) of the dynamic trajectories were sampled at 1 ps intervals. This procedure (summarized in Figure 2) was carried out for each polymer/water structure listed in Table 1. The number of different λ's at which configurations of the polymer/water systems were sampled was set to six, with λ-dependent force fields for $\lambda = 1.0$, $\lambda = 0.8$, ..., and $\lambda = 0.0$. The configurations sampled with the λ-dependent force fields were used to evaluate the functional form of the derivative $\partial\tilde{U}_{pot}(\lambda)/\partial\lambda$ (see eq 4 of ref 20).

The frames collected during the MD simulations with the $\lambda = 0$ force field were further used for calculating the excess chemical potential of noble water in amorphous polymer microstructures by use of the Widom's particle-insertion method. As already described in the companion paper,[20] we generate a three-dimensional uniformly spaced $30 \times 30 \times 30$ grid inside the simulation boxes and perform noble water insertion on all grid points. The excess chemical potential of noble water is then obtained through eq 3 of ref 20.

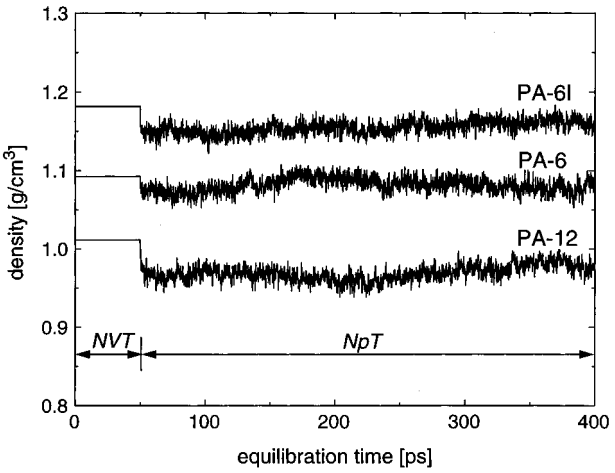

Figure 3. Density vs time during equilibration of polyamide systems containing 20 wt % water. The curves show instantaneous values sampled at 1 ps intervals.

Results and Discussion

Density. All polymer/water systems studied were initialized with the density of the amorphous dry polymer as described in the previous section. Due to the influence of the water molecules, a change of the system density during equilibration under constant-*NpT* conditions is expected and the density of the polyamide/water systems was monitored to follow the equilibration progress. Three typical curves of density vs time during the equilibration are shown in Figure 3. After the initial 50 ps of *NVT*-MD, the density decreases instantaneously upon changing to *NpT*-MD and starts fluctuating. One cannot expect truly equilibrated systems (even after much longer equilibration times), but after 400 ps all systems seem to be sufficiently equilibrated in their local minima in configuration space, as indicated by the small drifts in density observed during the final 100 ps of *NpT* equilibration; for all polyamide/water structures this drift is less than 3×10^{-4} g cm^{-3} ps^{-1}. However, the short equilibration times have to be taken into consideration; the calculated properties might depend on the specific polymer configuration, and sampling of independent structures is necessary. We investigated this influence exemplarily for two systems: PA-6 containing 20 wt % water and PA-12 containing 2 wt % water.

The system densities after equilibration of all polyamide/water systems studied are compared in Figure 4. While the precision of the "data" is not sufficient to yield a definitive correlation between water content and density, it seems that a linear combination rule (by weight fraction) is a reasonable approximation for the density of our polyamide/water systems. The densities of equivalent structures that were generated independently are within 3% and in the same range as the deviations of the densities of the structures from a linear-combination rule. Nevertheless, it is important to maintain each individual systems "natural" density, because this quantity strongly influences the results obtained by Widom's particle insertion, as will be shown in the next section.

Excess Chemical Potential. Applying the combination of thermodynamic integration and Widom's particle-insertion method, as introduced in the previous paper,[20] we calculated the excess chemical potential of water dissolved in the different polyamide/water systems. An overview of the estimated values of both steps of the calculation for all polyamide/water systems investigated is given in Table 2. For all systems, the main contribution to the excess chemical potential

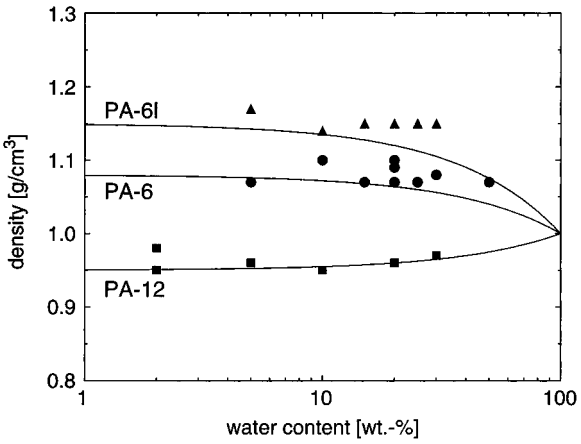

Figure 4. Density after equilibration as a function of the water content of the polyamide/water systems investigated (lines are for a linear combination rule, by weight fraction). The dry-polymer densities were taken from equilibrated structures calculated using identical simulation protocols ($\rho_{PA\text{-}6}$ = 1.08 g/cm^3, $\rho_{PA\text{-}12}$ = 0.95 g/cm^3, and $\rho_{PA\text{-}6I}$ = 1.15 g/cm^3).

Table 2. Calculated Results for Various Polyamide/Water Structures[a]

	water content (wt %)	$\Delta A^{ex}_{TI}/N_{H_2O}$ (kJ/mol)	ρ (g/cm^3)	μ^{ex}_{WI} (kJ/mol)
PA-6	5	−27.8(0.2)	1.07	+1.2(0.1)
	10	−26.3(0.2)	1.10	+2.0(0.2)
	15	−24.4(0.1)	1.07	+0.5(0.1)
	20	−23.8(0.1)	1.07	+0.4(0.1)
	20	−24.0(0.1)	1.10	+1.0(0.1)
	20	−24.5(0.1)	1.09	+0.8(0.1)
	20	*−24.1(0.4)*	*1.09(0.1)*	*+0.8(0.4)*
	25	−23.9(0.1)	1.07	+0.1(0.1)
	30	−23.6(0.1)	1.08	+0.2(0.1)
	50	−22.8(0.1)	1.07	−0.9(0.1)
PA-12	2	−23.5(0.4)	0.95	+1.0(0.1)
	2	−20.5(0.4)	0.95	+1.4(0.1)
	2	−23.0(0.4)	0.98	+2.2(0.1)
	2	*−22.3(1.9)*	*0.96(0.1)*	*+1.5(0.7)*
	5	−20.8(0.3)	0.96	+1.3(0.1)
	10	−20.9(0.2)	0.95	+0.8(0.1)
	20	−21.4(0.1)	0.96	+0.3(0.1)
	30	−20.9(0.1)	0.97	−0.2(0.1)
PA-61	5	−27.5(0.2)	1.17	+2.2(0.1)
	10	−25.1(0.2)	1.14	+0.4(0.1)
	15	−25.0(0.1)	1.15	+1.0(0.1)
	20	−24.9(0.1)	1.15	+0.7(0.1)
	25	−23.6(0.1)	1.15	+0.3(0.1)
	30	−23.7(0.1)	1.15	+0.3(0.1)
H_2O	100	−22.2(0.2)	1.00	−1.6(0.1)

[a] The numbers in parentheses give the standard error of the simulations calculated by assuming uncorrelated data. The numbers in italics give the average of multiple calculations with the same composition and (in parentheses) the associated standard errors.

originates from the scaling of nonbonded interactions during thermodynamic integration. Due to the fact that our systems contain many polar groups, the Coulombic interactions in real water strongly dominate the Lennard-Jones energies. The Coulombic interactions of the water molecules are completely eliminated during the first step (thermodynamic integration) and cause the large change in Helmholtz energy. The excess chemical potential calculated in the second step by Widom's particle-insertion method essentially only represents the contribution of the oxygen−oxygen Lennard-Jones interactions remaining after nonbonded interaction scaling.

For water dissolved in PA-6, the difference in Helmholtz energy due to the transformation of bulk water to noble water becomes less negative with increasing water

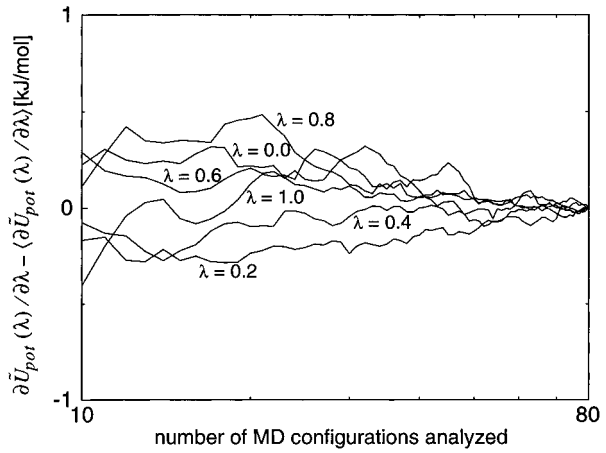

Figure 5. Convergence of the derivative of the potential energy with respect to λ for different λ, in the PA-12 system containing 30 wt % water.

content (see Table 2). The values calculated by thermodynamic integration for the PA-6/water systems are all lower than the corresponding ones for pure water (also given in Table 2 for comparison). Nearly the same principal behavior can be observed for water dissolved in PA-6I. Against this, the difference in Helmholtz energy estimated for water dissolved in PA-12 does not evolve uniformly; for some water contents it is above, for others below the corresponding value of the pure-water system.

Since only the nonbonded interactions of the water molecules are scaled during thermodynamic integration (all polymer atom interactions remain unchanged), the functional form of the derivative of the potential energy with respect to λ equals that of neat water (see Figure 5 in ref 20). The nearly linear behavior of $\partial \tilde{U}_{\mathrm{pot}}(\lambda)/\partial\lambda$ at higher values of λ is also observed for the polyamide/water systems (not shown) and gives credence to our simplification to only six force fields.

The convergence of the derivatives of the potential energies using different λ-dependent force fields is much faster than for the pure-water system. Figure 5 displays a typical example of the convergence behavior of the derivative of the potential energy with respect to λ (PA-12 system, 30 wt % water content). This convergence behavior seems to be satisfactory if one considers the deviations of the Helmholtz energy between polymer/water structures of equal composition (Table 2).

In contrast to the large contribution of the thermodynamic integration, the excess chemical potential of noble water determined by Widom's particle-insertion method contributes less than 10% to the total excess chemical potential of water (Table 2). For all three polyamide types (PA-6, PA-12, and PA-6I), two factors influencing the excess chemical potential of noble water can be identified: (i) The excess chemical potential of noble water decreases with increasing water content, as shown in Figure 6. This can be explained by the increasing "empty" space in the system left by the increasing number of hydrogen atoms "annihilated" during thermodynamic integration. (ii) For systems with identical composition, the density largely determines the value of the excess chemical potential of noble water. The higher the density, the lower the insertion probability and the higher the excess chemical potential of noble water dissolved in the polymer system (see PA-6, 20 wt % water content, Table 2). The latter effect has a stronger influence, as can be seen from the PA-6 systems containing 5 and 10 wt % water, respectively. Deviations from this general behavior occur and might be explained by other features, e.g., the inhomogeneity of "holes" that contribute to the excess chemical potential.

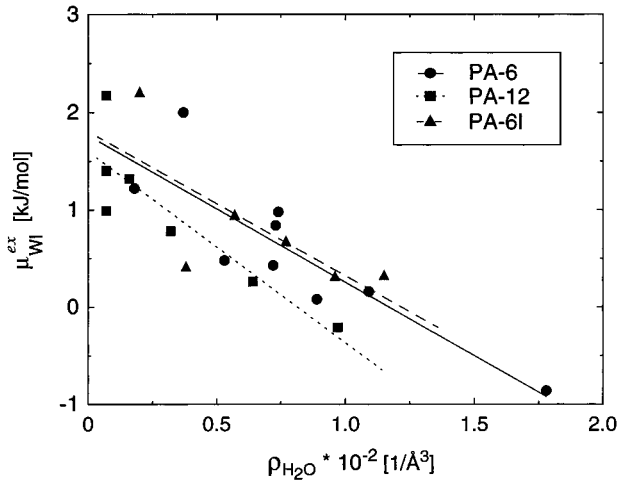

Figure 6. Excess chemical potential of noble water in the polyamide/water systems calculated by Widom's particle-insertion method, plotted against the number density of the water molecules. Lines are linear fits intended as guides to the eye.

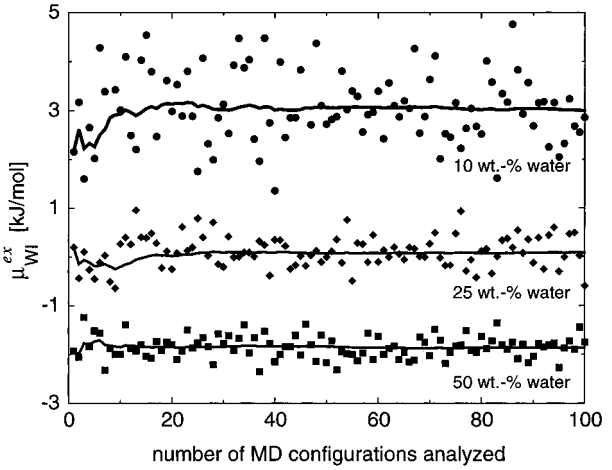

Figure 7. Excess chemical potential of noble water, calculated by Widom's particle-insertion method, in PA-6 systems containing 10, 25, and 50 wt % water, respectively. The representation is simplified by a shift of the results for 10 wt % by +1 kJ/mol and those for 50 wt % by −1 kJ/mol.

Figure 7 displays the convergence of the excess chemical potential of noble water calculated for three PA-6/water structures containing 10, 25, and 50 wt % water, respectively. For all systems the excess chemical potential of noble water has effectively approached its final value already after 40 ps MD sampling time. Furthermore, Figure 7 shows the decreasing scattering of the single values of the excess chemical potential with increasing water content; the higher the water content of the PA/water system, the larger the "empty" space in the system created by nonbonded interaction scaling, and the larger the Boltzmann factor relevant for Widom's insertion (see eq 3 in ref 20). This effect improves the statistics of insertions in one MD frame. Taking the magnitude of the Boltzmann factor contribution to eq 3 in ref 20 as a measure of "emptiness," we note that at 10 wt % water, 7% of all 27 000 grid points contribute Boltzmann factors larger than 10^{-10}, while at 25 wt %

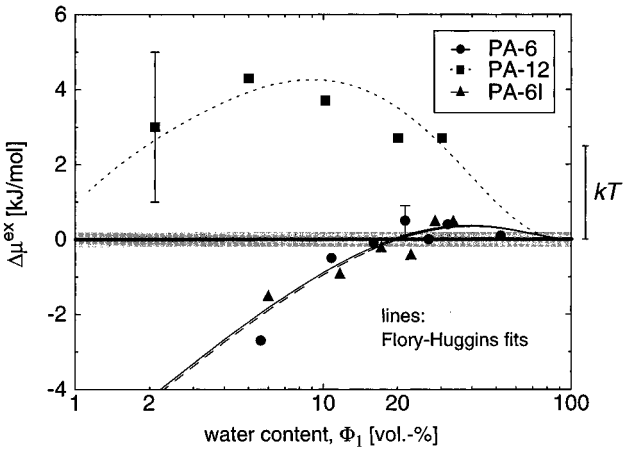

Figure 8. Calculated difference in excess chemical potential of water dissolved in amorphous polyamide microstructures and pure water at 300 K. The error bars indicate the standard error of the mean values calculated from three microstructures. The shadowed area denotes the standard error of the pure water calculation. The curves represent the Flory−Huggins expression with the fitted $\chi(\phi_1)$ (straight lines in Figure 9).

water this measure increases to 12% and, finally, to 16% at 50 wt % water.

Sorption Behavior. According to eq 1, the sorption behavior of the polymer systems submerged in neat water can be determined by looking at the difference between the excess chemical potential of water dissolved in the polymer microstructures and that of pure water. The excess chemical potential of water dissolved in the polymer structures is calculated as the sum of the intermediate results (thermodynamic integration and Widom's particle-insertion method) listed in Table 2. The excess chemical potential for pure water, the reference state, was taken as $\mu^{ex}_{H_2O} = -23.8$ kJ/mol. As described in detail in the companion paper,[20] this value was calculated using the same method and the same number of values for λ as for the polymer water systems considered here. Internal degrees of freedom were taken into account in all calculations. The calculated values for the difference in excess chemical potential are shown in Figure 8.

In the case of PA-6, the differential excess chemical potential is clearly negative for 5 and 10 wt % water. For higher water contents, the calculated difference is positive or within the error bar of the pure water system, indicating that the system would prefer to lessen its water content. This interpretation agrees well with experimental measurements on PA-6 that report the equilibrium water content after exposure to water at 293 K between 8 and 11 wt %, depending on the crystallinity of the specimen.[25,28,29] Extrapolation of these experimental results to zero crystallinity determines the water sorption of pure amorphous PA-6 to about 15 wt % water in surprisingly good agreement with our calculated data. However, it has to be pointed out that this simple linear extrapolation might not properly represent the complex situation in semicrystalline polymers; although the crystalline domains are probably not accessible to the small molecules, they may affect the packing of the amorphous chains. (Rogers et al.[27] considered crystallites as giant cross-linkages leading to unfavorable entropy effects, which limit the maximum swelling and sorption in the semicrystalline material.)

PA-6I exhibits nearly the same sorption behavior as PA-6 in our calculations (Figure 8). This agrees well with the assumption that water sorption of polyamides is mainly determined by the amide group concentration of the system, which is practically equal in the case of PA-6 and PA-6I. Since PA-6I allows measurements on purely amorphous structures, the experimental results can be compared unequivocally with the results on our model systems. The equilibrium water content of PA-6I is measured as 6 wt % water at 301 K,[26] smaller than the value that can be estimated from our calculated excess chemical potentials.

Against this, PA-12 shows a completely different sorption behavior. The difference of the excess chemical potential of water dissolved in PA-12 and neat water is positive for all PA-12/water microstructures investigated, as shown in Figure 8. These results suggest that the smallest water content investigated is higher than the equilibrium water content of PA-12. This conclusion is in reasonable agreement with experiments that report the saturation point of water in PA-12 around 1.8 wt %.[25,28]

Parenthetically, we would like to note that the calculated equilibrium water content is not a simple function of the concentration of C═O or N−H groups (or both) in the poly-amides. For PA-6 and PA-6I, equilibrium sorption is reached at ca. 1.5 water molecules per amide group, while for PA-12, ca. 0.05 water molecules per amide group can be accommodated. Inspecting the experimental values only would lead to the same conclusion: it is not a simply rationalizing function of the amide group concentration that determines equilibrium sorption.

The standard errors given for the mean of three independent calculations at 20 wt % water in PA-6 and 2 wt % water in PA-12 give an impression of the accuracy of our two-step method. For the high water content, the standard error of the mean is about 0.4 kJ/mol, considerably smaller than kT. The results are averages over many water molecules that form a continuous water cluster inside the simulation box. The influence of the different polymer structures disappears. On the other hand, for small water contents, such as 2 wt % water in PA-12, the results are more dependent on the specific model structure since most interactions are between water and the polymer. On the time scale of our simulations, it is not possible to sample the configuration space of the polymer chains; it is also doubtful if that of the water molecules is exhaustively scanned. Furthermore, there are only few water molecules inside the system, leading to less expedient statistics than for the high-water-content structures. A water content of 2 wt % has to be regarded as the lower bound for application of our method.

Polymer/Solvent Interaction. Traditionally, polymer/solvent systems have been described by the Flory−Huggins theory,[31,32] which was introduced for the description of mixtures whose molecules differ greatly in size. This theory uses a lattice model to account for the entropy effect of mixing and requires the interaction parameter χ for the mixing enthalpy. According to this theory the excess chemical potential of a solvent dissolved in a polymer matrix of infinite molecular weight can be written as[31]

$$\Delta\mu^{ex} = RT[\ln(\Phi_1) + (1 - \Phi_1) + \chi(1 - \Phi_1)^2] \quad (2)$$

with Φ_1 being the volume fraction of solvent (water) in the polymer matrix, χ the parameter related to the interaction Helmholtz energy of the first neighbors, R the universal gas constant, and T the temperature. Although χ was originally introduced as a system constant, many experimental measurements have shown

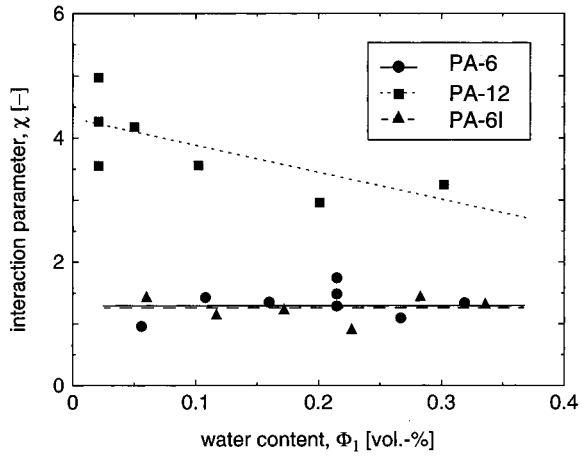

Figure 9. Values for the polymer/solvent interaction parameter χ at 300 K, calculated from the simulated differential excess chemical potentials, as a function of the water content of the polyamide/water system. Lines are linear fits to the data.

this parameter to be concentration dependent for a successful fit.

Equation 2 makes it feasible to determine the interaction parameter χ from our simulations of $\Delta\mu^{ex}$. This analysis allows the investigation of the functional dependence of χ on the solvent concentration by plotting χ as a function of the water content, as shown in Figure 9. For PA-6 and PA-6I the interaction parameter χ exhibits a nearly concentration-independent behavior; χ can be estimated as roughly 1.3 for PA-6 and PA-6I, respectively. For the PA-12 system our calculations show a concentration-dependent interaction parameter. Here we use a linear fit for the description of the interaction parameter χ: $\chi = 4.3(1 - \Phi_1)$. Using these χ parameters and eq 2, smooth and continuous curves of $\Delta\mu^{ex}$, consistent with the Flory−Huggins theory, can be drawn; they were also plotted in Figure 8. They fit our simulated results for the difference in excess chemical potential very well. Using these curves as a course interpolation and smoothing tool, one would obtain sorption limits of 18 wt % for PA-6, of 17 wt % for PA-6I, and of 0.5 wt % for PA-12, respectively.

Conclusion

The calculations presented clearly show it possible to combine thermodynamic integration and Widom's particle-insertion method in order to estimate the excess chemical potential of water in dense polyamide/water microstructures. The calculations give an approximation to the degree of sorption of water into the amorphous polymer, in reasonable agreement with experimental data. This is even possible for systems where the macromolecule is described by identical atom types in the force field, the difference being only in their proportion, as in the case of PA-6 and PA-12. The force field, the combination of its expressions and parameters, seems to be accurate enough to account for the effects of the differences in the amide group concentration of these systems. On the other hand, we estimate PA-6 and PA-6I to have almost identical sorption behavior, in contrast to reality. These systems show nearly identical amide group concentrations, but different chemical structures. Apparently, the influence of the aromatic ring structure is not described in sufficient detail by the force field.

All differential excess chemical potentials calculated during this study are different from zero only within a few kJ/mol. As a consequence, our interpretations have to rely on very small energy differences. Nevertheless, we can reproducibly distinguish between different sorption behaviors of similar polymers such as PA-6 and PA-12, and we can determine the equilibration sorption of different polyamides at experimental densities in a thermodynamically sound way.

Since we have made no assumptions specific to polyamides or water, applications of our method to other systems containing small molecules in polymer matrices seem feasible. The only prerequisite is the definition of an appropriate nonbonded-interaction scaling scheme that ensures the reduction of the nonbonded interactions to a point where the density of the system is low enough so that Widom's particle-insertion method becomes successful.

Acknowledgment. We gratefully acknowledge support for B.K. from the Deutsche Forschungsgemeinschaft under Grant No. DFG Kn 417/1-1 and general financial support by EMS-Chemie AG, Domat/Ems, Switzerland. Generous amounts of computer time were provided by the Competence Centre for Computational Chemistry (C4) of the ETH Zürich. We also acknowledge the inspiring and thougthful discussions with Andrei A. Gusev.

References and Notes

(1) Takeuchi, H.; Okazaki, K. *J. Chem. Phys.* **1990**, *92*, 5643.
(2) Takeuchi, H.; Roe, R.-J.; Mark, J. E. *J. Chem. Phys.* **1990**, *93*, 9042.
(3) Mueller-Plathe F. *Macromolecules* **1991**, *24*, 6475.
(4) Gusev, A. A.; Suter, U. W. *Phys. Rev. A* **1991**, *43*, 6488.
(5) Sok, R. M.; Berendsen, H. J. C.; van Gunsteren, W. F. *J. Chem. Phys.* **1992**, *96*, 4699.
(6) de Pablo, J. J.; Laso, M.; Suter, U. W. *J. Chem. Phys.* **1992**, *96*, 6157.
(7) de Pablo, J. J.; Laso, M.; Suter, U. W. *Macromolecules* **1993**, *26*, 6180.
(8) Pant, P. V.; Boyd, R. H. *J. Chem. Phys.* **1993**, *98*, 9895.
(9) Gusev, A. A.; Arizzi, S.; Suter, U. W.; Moll, D. J. *J. Chem. Phys.* **1993**, *99*, 2221.
(10) Gusev, A. A.; Suter, U. W. *J. Chem. Phys.* **1993**, *99*, 2228.
(11) Mueller-Plathe, F.; Rogers, S. C.; van Gunsteren, W. F. *J. Chem. Phys.* **1993**, *98*, 9895.
(12) Han, J.; Boyd, R. H. *Macromolecules* **1994**, *27*, 5365.
(13) Tamai, Y.; Tanaka, H.; Nakanishi, K. *Macromolecules* **1994**, *27*, 4498.
(14) Tamai, Y.; Tanaka, H.; Nakanishi, K. *Macromolecules* **1995**, *28*, 2544.
(15) Gee, R. H.; Boyd, R. H. *Polymer* **1995**, *36*, 1435.
(16) Gusev, A. A.; Suter, U. W.; Moll, D. J. *Macromolecules* **1995**, *28*, 2582.
(17) Ralston, A. R. K.; Denton, D. D.; Bicerano, J.; Moll, D. *Comput. Polym. Sci.* **1996**, *6*, 15.
(18) Bicerano, J. Moll, D. J. *Comput. Polym. Sci.* **1996**, *6*, 117.
(19) van der Vegt, N. F. A., Briels, W. J., Wessling, M., Strathmann, H. *J. Chem. Phys. 1997, 105, 8849.*
(20) Knopp, B.; Suter, U. W.; Gusev, A. A. *Macromolecules* **1997**, *30*, 6107.
(21) Insight 3.0.0; Discover 2.9.7; Amorphous Cell 8.0.0; Biosym/MSI, Inc., San Diego, CA, 1991.
(22) Berendsen, H. J. C.; Postma, J. P. M.; van Gunsteren, W. F.; DiNola, A.; Haak, J. R. *J. Chem. Phys.* **1984**, *81*, 3684.
(23) Verlet, L. *Phys. Rev.* **1967**, *159*, 98.
(24) Theodorou, D. N.; Suter, U. W. *Macromolecules* **1985**, *18*, 1467.
(25) *Polymer Handbook*, 3rd ed.; Brandrup, J., Immergut, E. H., Eds.; Wiley: New York, 1989.
(26) Ebert, M.; Hewel, M. Personal communication, 1997, EMS-Chemie, Domat-Ems, Switzerland.
(27) Rogers, C. E.; Stannett, V.; Szwarc, M. *J. Phys. Chem.* **1959**, *63*, 1406.
(28) Song, J.; Ehrenstein, G. W. *Kunststoffe* **1990**, *80*, 722.
(29) *Kunststoff-Handbuch, Bd. VI, Polyamide*; Vieweg, R., Müller, A. Carl, Eds.; Hanser Verlag: München, 1966; p 470.
(30) Franck, A.; Biederbick, K. *Kunststoff-Kompendium*, 3. Aufl.; Vogel Buchverlag: Würzburg, 1990.
(31) Flory, P. J. *J. Chem. Phys.* **1942**, *10*, 51.
(32) Huggins, M. L. *J. Chem. Phys.* **1941**, *9*, 440.

MA970384M